

# Cancer detection based on electrical impedance spectroscopy: A clinical study

Sepideh Mohammadi Moqadam<sup>1</sup>, Parvind Kaur Grewal<sup>1</sup>, Zahra Haeri<sup>1</sup>, Paris Ann Ingledew<sup>2</sup>, Kirpal Kohli<sup>2</sup>, and Farid Golnaraghi<sup>1,3</sup>

1. School of Mechatronic Systems Engineering, Simon Fraser University, 250–13450 102nd Avenue, Surrey, Canada, BC V3T 0A3
2. BC Cancer Agency Provincial Health Services Authority, 13750 96 Ave, Surrey, Canada, BC V3V 1Z2
3. E-mail any correspondence to: [mfgolnar@sfu.ca](mailto:mfgolnar@sfu.ca)

## Abstract

An electrical Impedance based tool is designed and developed to aid physicians performing clinical exams focusing on cancer detection. Current research envisions improvement in sensor-based measurement technology to differentiate malignant and benign lesions in human subjects. The tool differentiates malignant anomalies from nonmalignant anomalies using Electrical Impedance Spectroscopy (EIS). This method exploits cancerous tissue behavior by using EIS technique to aid early detection of cancerous tissue.

The correlation between tissue electrical properties and tissue pathologies is identified by offering an analysis technique based on the Cole model. Additional classification and decision-making algorithm is further developed for cancer detection. This research suggests that the sensitivity of tumor detection will increase when supplementary information from EIS and built-in intelligence are provided to the physician.

**Keywords:** Electrical Impedance (EI); electrical Impedance spectroscopy (EIS); Cole model; early cancer detection; fitting-model; LAD error function

## Introduction

Cancer is a disease, which consists of division of abnormal cells without control. Blood and lymph systems can help cancerous cells spread to other parts of the body [1, 2]. Skin cancer is the most common of all cancer types. Screening for skin cancer is usually made by visual inspection of the lesions. Due to its subjective nature, the clinical accuracy of this screening can range from good to poor depending on the experience of the clinician. It is

desirable to replace this subjective process with a non-invasive, reliable, simple, and objective technique with high sensitivity and specificity. There is a high chance of cure for skin cancer in its early stages. Examinations are essential due to this reason [3].

One promising avenue of research for diagnosing skin cancer accurately, non-invasively, and potentially at an earlier stage is Electrical Impedance Spectroscopy (EIS) [4,5]. The living cell's membrane is semi-permeable which means it behaves similar to an electrochemical membrane. This feature causes some ions to pass through the membrane while it blocks other ones. Also, the resistive characteristics of the intracellular and extracellular area is due to existence of electrolytes. Calculating bioimpedance of tissue allows us to consider both capacitive and resistive characteristics of the tissue [6,7].

Bearing in mind the commonality of skin cancer and the high survival rate if diagnosed at early stages, there is a need to develop a new methodology to replace the traditional subjective process. Various studies have shown a statistically significant difference in electrical impedance between cancerous tissue and normal tissue [8–11]. Consequently, we developed a device consisting of electrical impedance electrodes in this study. The overall purpose of this paper is to utilize the multi-frequency electrical impedance spectroscopy (EIS) system. EIS, or opposition to the flow of an electric current through body tissues, is a commonly used method for estimating body composition. For example, EIS analysis is used in the measurement of total body fat. EIS analysis measures body

tissue resistance (due to extracellular fluid) and capacitance (due to cell membranes) by recording a voltage drop in the applied current. Cancerous tissue has been shown to have different electrical properties than normal tissue. By passing mild electrical signals of different frequencies through body tissue and measuring resistance, the tissue can be “mapped” and abnormal lesions identified [11–14].

The overall purpose of this paper is to utilize the multi-frequency electrical impedance spectroscopy (EIS) system.

## Materials and methods

### Experimental setup for the *in-vivo* electrical study

This study was performed with a bioimpedance measurement setup. The bio-impedance measurements, which will be explained in the following have been performed on both the left and right forearms and biceps of 21 subjects.

*In-vivo* experiments were performed on left and right forearm and bicep of eleven healthy and ten cancerous human subjects. For the *in-vivo* bioimpedance experiment, two Ag/AgCl electrodes were integrated into a probe. Electrical impedance electrodes, along with temperature sensors, were integrated into an enclosure by the computer aided design software SolidWorks. After that, the prototype was developed using a 3D printer and the rapid prototyping technique. In this design, which is shown in Figure 2, two Ag/AgCl electrodes, as well as six temperature sensors, were integrated into the probe [15]. The temperature sensors were used for another study, therefore the results of the temperature sensors are not presented in this paper [15]. The probe was designed in a way that the electrodes were at 2-centimeter distance. The input units for EIS play an important role in this system. Several factors that the input unit should cover are sensitivity, dynamic range, and speed. In order to address all of the preceding mentioned factors, the Model HF2TA trans-impedance amplifier from Zürich Instruments was used in this study. The frequency sweep range is selected from 300 Hz to 1 MHz with 50 step-points, which is enough to create fitted Nyquist plots and extract electrical properties of the tissue under test. Most of the patients in this study suffered from stage 2 or 3 skin cancer. Therefore, their tumors were 1-4 mm deep with ulceration or larger than 4 mm without ulceration (Figure 1).

In these cases, the area under study was the deeper living layers of the skin. As high frequency measurements reflects the deeper layers of skin [16], the chosen frequency range was suitable for capturing the cancer of the volunteer subjects.

The designed probe works in the safe current range of 20  $\mu$ A. The probe’s supplier system has an isolation amplifier, which isolates the probe from power line and guarantees safety. The four features of accurate phase shift, high dynamic reserve, zero drift and orthogonality

make this device a good choice over the other valid analog devices. The frequency response can also be derived from noisy and low voltage sets by using this setup.

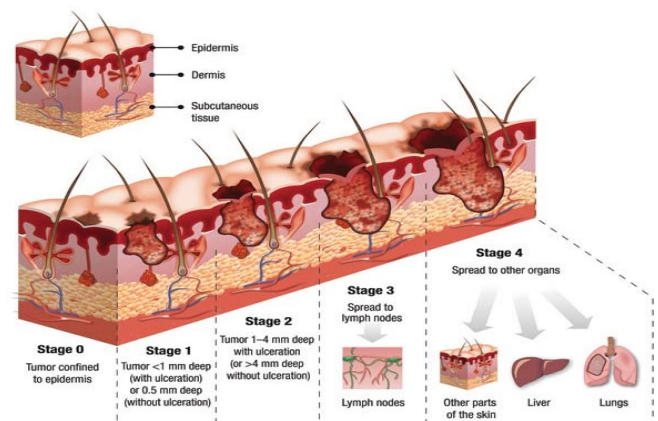


Figure 1: Skin cancer stages (source: teleskin.org)

A special area was considered for the gel (gel is used to fill the gap between sensors and skin) so that the used gel of each electrode is not mixed with the gel of the other electrode. In spite of the design of the electrode positions in such a way that the gels cannot be mixed, the electrodes were in a good contact with the tissue. As the focus of this study is not the stratum corneum, the gel influence on the measurements is neglected. The details of the probe design can be seen in Figure 3.

To have consistency in the results, the tests were performed on contralateral sites of the body. For bicep and forearm tests, the probe was placed at a distance 8 cm from elbow and wrist respectively. The finger TPS pressure sensor is designed to be worn over the examiner’s index finger to apply constant pressure over the probe (see Figure 4). The applied pressure was held constant by the examiner monitoring the pressure value from the Chameleon TVR software. The force level was chosen in a way that the pressure value was tolerable by the human subjects (2.5 N). The *in-vivo* admittances were measured at the force level in three trials and recorded for further analysis.

### Experimental setups in *in-vivo* cancer detection study

This section describes the experimental setup used for the *in-vivo* cancer detection study. The main purpose of this study was to utilize the electrical impedance spectroscopy as a means for cancer detection. Since the malignancy changes the tissue structure, the tissue electrical properties in the malignant tissue will also be different from the electrical properties of healthy tissue. This study was a collaborative research project with BC cancer agency (BCCA). The primary purpose of this study was to test EIS over breast cancerous subjects. However, the team oncologists’ suggestion was to test the method on skin tumors due to the sensitivity involved in breast cancer patients. This study was performed under the UBC BCCA Research Ethics Board under Dr. Paris Ann Ingledew as the Principal Investigator and REB Number H13- 02887. Ethics

approval for conducting this study was given by the UBC BCCA Research Ethics Board and SFU Ethics Board. The title of the ethic approval is: “Electrical Impedance Analysis of Malignant and Benign Skin Tissue: Effects of Temperature and Pressure”.

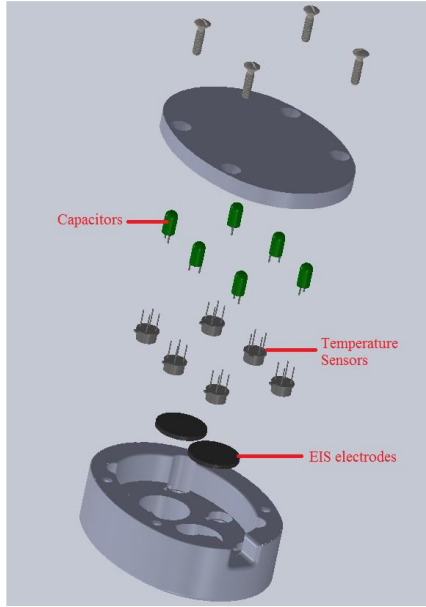


Figure 2: The exploded view of the probe containing electrical impedance electrodes as well as temperature sensors.



Figure 3: Design of the probe in SolidWorks and the prototype



Figure 4: Use of probe and the pressure sensors over human tissue

In this study, ten cancerous subjects were recruited. The study was performed over malignant skin tumors with their contralateral healthy tissue as the control. The details of

the skin cancerous subjects, their age, sex, type of tumor and tumor position are listed in Table 1.

Table 1: Case studies recruited for testing the proposed method on cancerous subjects and their information

Case Study No.	Age	Sex	Tumor Type	Tumor Position
Subject 1	90	Female	BCC (Basal Cell Carcinoma)	Left side of nose along sidewall
Subject 2	97	Female	SCC (Squamous Cell Carcinoma)	Left cheek center
Subject 3	81	Male	SCC (Squamous Cell Carcinoma)	Right Temple of head
Subject 4	93	Female	SCC (Squamous Cell Carcinoma)	Left cheek
Subject 5	87	Female	BCC (Basal Cell Carcinoma)	Left cheek under the eye
Subject 6	93	Female	BCC (Basal Cell Carcinoma)	Left mid neck
Subject 7	87	Male	BCC (Basal Cell Carcinoma)	Right cheek
Subject 8	92	Male	SCC (Squamous Cell Carcinoma)	Forearm
Subject 9	66	Female	BCC (Basal Cell Carcinoma)	Upper left cheek
Subject 10	65	Male	BCC (Basal Cell Carcinoma)	Left nasal wing

The electrical properties of tissue change with compression [17]. Thus, in this study, the force sensors was utilized to monitor the amount of applied pressure over the tissue, so as to apply the same amount of pressure on all subjects and hence have consistency in results.

#### Mathematical modeling of admittance data

Various models and circuit theories have been proposed for modeling the multi-frequency electrical impedance data. These models consider the tested tissue as a circuit containing some resistances and capacitances. In this study parameter mapping of EIS will be presented using the popular model: the “Cole model” in the form of admittance. The structure of this circuit and its constitutive mathematical equations are explained as follows:

#### Cole model (in the form of admittance)

The circuit of the Cole model is illustrated in Figure 5. The admittance of human tissue can be expressed by the Cole equation (Eq.1) in the form of admittance proposed by Liu et al. [18,19]

$$Y = G + jB = G_{\infty} + \frac{G_0 - G_{\infty}}{1 + \left(\frac{jf}{f_{yc}}\right)^{\alpha}} = \frac{1}{Z} \quad \text{Eq.1}$$

where  $Y$  is the whole admittance,  $G$  is the conductance and  $B$  is the susceptance.  $G_0$  is the admittance at zero driving frequency,  $G_\infty$  is the admittance when the driving frequency is infinity (it should be known that  $G_0$  and  $G_\infty$  are only valid within one single dispersion),  $f$  is the driving frequency,  $f_{yc}$  is the frequency at which the imaginary part of the admittance reaches its maximum and  $\alpha$  is the dispersion parameter.

As stated by Liu *et al.* [20], the equation of admittance can form the equation of a circle, and thus plotting the imaginary part of admittance (susceptance) versus the real part of admittance (conductance) in a complex plane, results in a circular arc as shown in Figure 6.

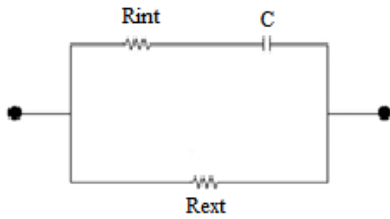


Figure 5: The Debye case of the Cole model circuit ( $\alpha=1$ ).

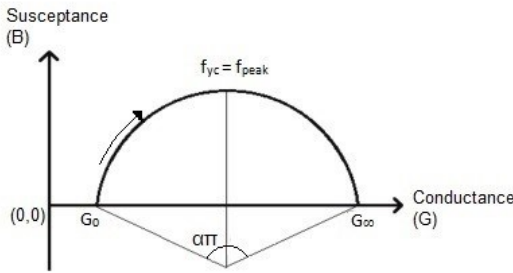


Figure 6: Imaginary part of admittance versus its real part (Cole plot).

The low-frequency region is affected by the extracellular environment and the high-frequency region is influenced by the intracellular space. In other words, since the cell membranes have a high capacitance, currents at low frequency cannot penetrate into the cell and must pass around the cells and go through the extracellular area. According to the Cole circuit, at low frequencies, open circuit occurs in the branch containing capacitance. Therefore, current flows only through the resistor called extracellular resistance. High frequency currents, on the other hand, have the ability to penetrate through cell membranes and other electronic barriers in the cell structure by polarisation. In the Cole circuit, the same behavior is observed at high frequencies in which the capacitor short circuit occurs and thus current flows through both resistances in parallel [21]. Based on these facts, the Cole model may represent the cellular properties of biological tissue in an efficient way, which is illustrated in Figure 7.

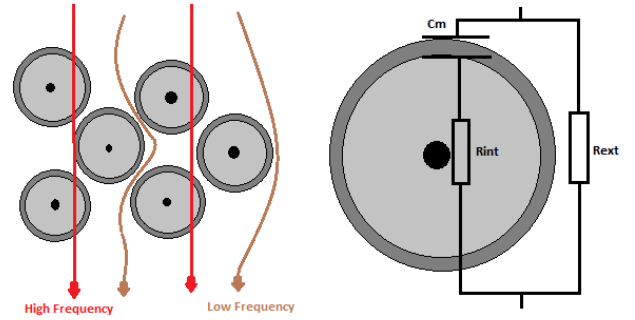


Figure 7: Paths of high and low frequency currents in a biological tissue.

### Parameter fitting of Cole-Cole model in form of admittance

The LAD method is an optimization method which minimizes the summation of the absolute errors which can be found by subtracting each data point from the fitted data as it is shown in Eq.2 [22].

$$\text{FitnessFunc.} = \min \sum |e_i| \quad \text{Eq.2}$$

Four Cole features ( $G_0$ ,  $G_\infty$ ,  $\alpha$ , and  $f_{yc}$ ) are extracted by this method. The Cole model models the tissue as a circuit including one resistor in series with one capacitor, and both in parallel with a resistor. The resistor and capacitor which are in series mimic the intracellular resistance ( $R_{int}$ ) and bulk membrane capacitance ( $C_m$ ) and the resistor in parallel with these two components mimics the extracellular resistance of tissue ( $R_{ext}$ ). All these three Cole circuit parameters can be calculated using Eq.3:

$$R_{ext} = R_0 \quad \text{Eq.3}$$

$$R_{int} = \frac{R_0 R_\infty}{R_0 - R_\infty}$$

$$C_m = \frac{1}{2 \pi f_c (R_{int} + R_{ext})}$$

$$\text{where } R_0 = \frac{1}{G_0}, R_\infty = \frac{1}{G_\infty} \text{ and } f = f_{yc} \alpha \sqrt{\frac{G_0}{G_\infty}}$$

### Results

Based on the experimental procedures and the mathematical modeling method explained before, the results of experiments and further mathematical analysis on the results are presented. Then the experimental results of healthy and cancerous subjects are compared.

### Validating the use of contralateral in-vivo sites as control

In this study, the use of contralateral sites of the body is proposed to be used as the control. Soft tissue is conductive, and the tissue conductivity is different in various types of tissues. Thus it is postulated that similar

cellular structure is leading to similar electrical behavior [12, 23]. Moreover, the electrical properties of malignant tissues are altered compared to healthy tissue due to the increased cellular water and sodium content, altered membrane permeability, and changed packing density and orientation of cells [24]. As a result, in this study it is proposed to use the contralateral sites of the body as control. This idea suggests that if the tested tissue is healthy, the changes in electrical properties of that tissue on its contralateral site will not be significant and if the tested tissue is tumorous, a significant change in the electrical properties will be observed. In this section, the changes of the electrical properties of healthy and cancerous human tissues, about their contralateral parts, are studied.

### Admittance results of contralateral sites in healthy subjects

To make a comparison, the bioimpedance measurements were conducted on the contralateral sites on biceps and forearms. The imaginary part of the admittance of each subject was plotted versus the real part of the admittance, thus the Nyquist plot of each subject was obtained. After that, the raw data were fitted into the Cole model and the corresponding electrical parameters were calculated. We compared the Nyquist plots of eleven healthy subjects' biceps and forearms as well as their contralateral Nyquist plots. As a result of the comparison, the contralateral sites of the body have almost the same Nyquist bioimpedance results.

### Admittance results of contralateral sites in tumorous subjects

The same procedure in presenting the healthy subjects' data was incorporated in this part; the imaginary part of admittance of each subject is plotted versus the real part of admittance, thus the Nyquist plot of each subject can be obtained. To compare the differences in admittances of tumorous and healthy tissues, the admittance of the tumorous part of each patient and the admittance of its contralateral healthy site were presented in the same Nyquist plot. After that, the raw data were fitted into the Cole model and the corresponding electrical parameters were calculated. In Figure 8, the Nyquist plots of the tumorous body parts of ten tumorous subjects as well as their contralateral healthy sites are illustrated and the results are visually comparable.

Figure 8 shows that the admittance Nyquist plots of contralateral sites in tumorous subjects significantly vary. As shown in this study, the use of electrical impedance of contralateral parts of body can be used as the control when performing tumor detection in human tissue. In this section, the electrical impedance spectra, measured from volunteer subjects, are used to train classification methods for automatic detection of malignancy.

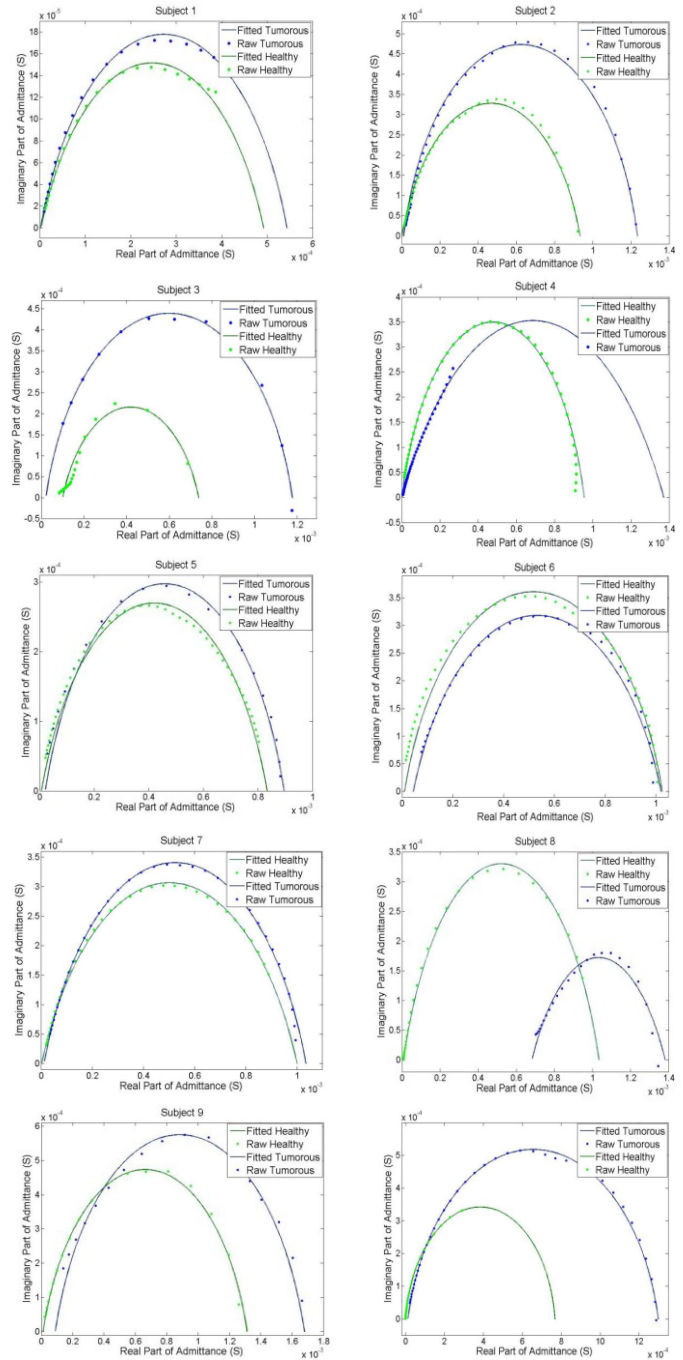


Figure 8: Admittance plot of the tumorous subjects and the contralateral healthy part.

Three classification methods are implemented on the raw data, the extracted features as well as the normalized features. Thereafter, the performance of each classification method on both raw and processed data are compared. Three different classifier techniques were used in this study: Naïve Bayes classifier with Gaussian distribution, Naïve Bayes classifier with Kernel distribution and support vector machine (SVM). Using electrical bioimpedance spectra of in-vivo tissue, the human subjects are classified into two classes: cancerous and healthy classes (10-fold cross validation, which is a popular choice of cross validation, was performed on the data).

A program was written in MATLAB for training and testing of NB classifiers (with Gaussian and Kernel

distribution) and SVM classifier. The three classification methods have been applied on the raw data, the extracted features and the normalized extracted features. The accuracy, sensitivity, specificity, cross validation error and the misclassification error or resubstitution error of each method are illustrated in

Figure 9 and Table 2.

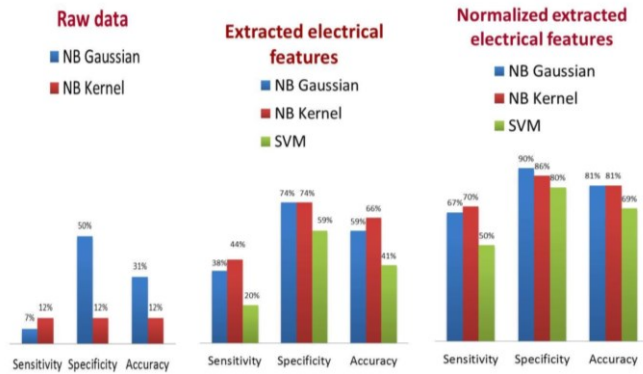


Figure 9: Comparison of the performance of 3 classification methods on the data.

Table 2: The performance of various classification methods on raw and processed data.

		Sensi- tivity %	Speci- ficity %	Accuracy %	Resubsti- tution %	Cross Vali- dation Error %
Raw Data	NB Gaussian	7.14	50	31.25	68.75	54.17
	NB Kernel	12.5	12.5	12.5	87.5	87.5
Extracted Features	NB Gaussian	38.46	73.68	59.38	40.63	31.2
	NB Kernel	44.44	73.91	65.63	34.38	33.3
	SVM	20	58.82	40.63	59.38	53.12
Normalized Extracted Features	NB Gaussian	66.67	90	81.25	18.75	16.67
	NB Kernel	70	86.36	81.25	18.75	13.12
	SVM	50	80	68.75	31.25	18.75

These results support the proposed idea of this research that the contralateral sites of body should have the same electrical properties unless there is a malignancy in one of the sites.

**Discussion**

In this study, the changes in electrical properties of living tissue were compared contra-laterally. The results illustrate the same behavior and the same linear correlation in contralateral parts of human subjects. This observation suggests that the correlation of electrical properties of one part of the body is the same as its contralateral part unless there is an abnormality in one of the contralateral parts. This comparison of electrical correlation of contralateral parts of the body can be considered as a method for diagnosis of tumor or any abnormalities within tissue.

Even though this study and method was developed for breast cancer detection, the experiments were conducted on biceps and forearms of healthy subjects and subjects with skin cancer. There were many limitations in performing human studies on healthy and cancerous breasts. High

sensitivity, which was involved in the breast cancer patients, made us perform the experiments on skin cancer patients. Based on a study performed by Grewal *et al.*, the electrical bioimpedance of bicep and forearm is the closest electrical bioimpedance to the breast tissue [11]

In this paper, which involves cancer detection using various classification techniques, 32 subjects (22 healthy body positions of 11 subjects and 10 cancerous subjects) were recruited for this study. The electrical admittance spectra of the 32 subjects were measured by a probe containing Ag/AgCl electrodes. The most commonly used bioimpedance model, the Cole model was then fitted to the data.

Due to high inter-subject variation in the electrical properties, it was proposed in this study to normalize the electrical properties of each subject. Since the electrical properties of biologic tissue are significantly dependent on the tissue structure [25], it was postulated that the electrical properties of any tissue with exact structure should be approximately the same. Since each subject’s left and right body parts have almost the same tissue structure, it was suggested that their multi-frequency admittance data and, therefore, their electrical properties should not be significantly different, unless there is a malignancy in one of the body parts. This hypothesis was statistically tested and the results were promising. The results revealed that the admittances and the Cole circuit equivalent electrical parameters of the contralateral sites in healthy subjects are not significantly different; however, the admittances and the Cole circuit equivalent electrical parameters of the lesions and their contralateral healthy sites are significantly different.

One of the challenges in the future study will be the depth of tumors; the tumors in skin cancer patients are not deep and they are usually on the surface of skin. The depth that the electrical current can penetrate to the tissue is half the distance between the electrodes [19]. Thus, for the purpose of testing the technology on skin cancer patients, a small distance between the electrodes was designed, so that most of the electrical current flowed through the tumor on the skin and the amount of penetration of current to the tissue was small. The probe can be redesigned and the distance between the electrodes can be increased to use the probe on breast tissue.

The concepts and results of this study can translate to breast cancer. This concept was tested on the skin and can be expanded to any tissue including breast tissue. This research group will validate this technology on breast cancer patients shortly.

**Acknowledgments**

The authors are thankful to all the participants in this research. Financial support for this project was provided in

part by the Natural Sciences and Engineering Research Council of Canada (NSERC).

## References

1. Haeri Z, Shokoufi M, Jenab M, Janzen R, Golnaraghi F (2016) Electrical impedance spectroscopy for breast cancer diagnosis: Clinical study. *Integr Cancer Sci Ther* 3:1–6. <https://doi.org/10.15761/ICST.1000212>
2. Nover AB, Jagtap S, Anjum W, Yegingil H, Shih WY, Shih W-H, Brooks AD (2009) Modern breast cancer detection: a technological review. *Int J Biomed Imaging* 2009:902326. <https://doi.org/10.1155/2009/902326>
3. Dermatology of Seattle. <http://dermatologyseattle.com/skincancer/?gclid=COTpzejUwNMCFQqnaQodhe0OWw>.
4. Beetner DG, Kapoor S, Manjunath S, Zhou X, Stoecker W V. (2003) Differentiation among basal cell carcinoma, benign lesions, and normal skin using electric impedance. *IEEE Trans Biomed Eng* 50:1020–1025. <https://doi.org/10.1109/TBME.2003.814534>
5. Glickman Y, Filo O, David M (2003) Electrical impedance scanning: a new approach to skin cancer diagnosis. *Ski Res Technol* 9:262–268. <https://doi.org/10.1034/j.1600-0846.2003.00022.x>
6. Polk C, Postow E (eds) (1996) *Handbook of biological effects of electromagnetic fields*, Second Edi. CRC Press LLC
7. Åberg P (2004) *Skin cancer as seen by electrical impedance*. PhD thesis, Karolinska institutet, Sweden.
8. Laufer S, Ivorra A, Reuter VE, Rubinsky B, Solomon SB (2010) Electrical impedance characterization of normal and cancerous human hepatic tissue. *Physiol Meas* 31:995–1009 <https://doi.org/10.1088/0967-3334/31/7/009>
9. Kim BS, Isaacson D, Xia H, Kao T-J, Newell JC, Saulnier GJ (2007) A method for analyzing electrical impedance spectroscopy data from breast cancer patients. *Physiol Meas* 28:S237-246. <https://doi.org/10.1088/0967-3334/28/7/S17>
10. Keshtkar A, Keshtkar A, Smallwood RH (2006) Electrical impedance spectroscopy and the diagnosis of bladder pathology. *Physiol Meas* 27:585–596. <https://doi.org/10.1088/0967-3334/27/7/003>
11. Morimoto T, Kimura S, Konishi Y, Komaki K, Uyama T, Monden Y, Kinouchi Y, Iritani T (1993) A study of the electrical bio-impedance of tumors. *J Invest Surg* 6:25–32. <https://doi.org/10.3109/08941939309141189>
12. Foster KR, Schwan HP (1989) Dielectric properties of tissues and biological materials: a critical review. *Crit Rev Biomed Eng* 17:25–104.
13. Emtestam L, Nicander I, Stenstrom M OS (1998) Electrical impedance of nodular basal cell carcinoma: a pilot study. *Dermatology* 197:313-31. <https://doi.org/10.1159/000018023>
14. Malich A, Fritsch T, Mauch C, Boehm T, Freesmeyer M, Fleck M, Anderson R KW (2001) Electrical impedance scanning: a new technique in the diagnosis of lymph nodes in which malignancy is suspected on ultrasound. *Br J Radiol* 74:42-47. <https://doi.org/10.1259/bjr.74.877.740042>
15. Shokoufi M, K Grewal P (2016) Periodic Dynamic Thermography for Breast Cancer Assessment. *J Bioeng Biomed Sci* 6:6–10. <https://doi.org/10.4172/2155-9538.1000181>
16. Martinsen ØG, Grimnes S, Haug E (1999) Measuring depth depends on frequency in electrical skin impedance measurements. *Ski Res Technol* 5:179–181. <https://doi.org/10.1111/j.1600-0846.1999.tb00128.x>
17. Moqadam SM, Grewal P, Shokoufi M, Golnaraghi F (2015) Compression-dependency of soft tissue bioimpedance for in-vivo and in-vitro tissue testing. *J Electr Bioimpedance* 6:22-32. <https://doi.org/10.5617/jeb.1489>
18. Liu R, Dong X, Fu F, You F, Shi X, Ji Z, Wang K (2007) Multi-frequency parameter mapping of electrical impedance scanning using two kinds of circuit model. *Physiol Meas* 28:S85-100. <https://doi.org/10.1088/0967-3334/28/7/S07>
19. Cole KS (1972) *Membrane, Ions and Impulses*, Univ. of California Press.
20. Moqadam SM (2015) *Tissue Characterization and Cancer Detection Based on Bioimpedance Spectroscopy*. MSc thesis, Simon Fraser University, Canada.
21. Chen K, Ying Z, Zhang H, Zhao L (2008) Analysis of least absolute deviation. *Biometrika* 95:107–122. <https://doi.org/10.1093/biomet/asm082>
22. Grewal PK (2014) *Multimodality based Tissue Classification Technique for Malignant Anomaly Detection*. PhD thesis, Simon Fraser University, Canada.
23. Morucci JP, Rigaud B (1996) Bioelectrical impedance techniques in medicine. Part III: Impedance imaging. Third section: medical applications. *Crit Rev Biomed Eng* 24:655–677.
24. Golnaraghi F, Grewal PK (2014) Pilot study: electrical impedance based tissue classification using support vector machine classifier. *IET Sci Meas Technol* 9:579–587.
25. Grimnes S, Martinsen ØG (2008) Geometrical analysis. In: *Bioimpedance Bioelectr. Basics*. Elsevier, pp 161–204. <https://doi.org/10.1016/B978-0-12-374004-5.00006-4>